Scientific Journal of Silesian University of Technology. Series Transport
Zeszyty Naukowe Politechniki Śląskiej. Seria Transport

Volume 124 **2024**

p-ISSN: 0209-3324

e-ISSN: 2450-1549

DOI: https://doi.org/10.20858/sjsutst.2024.124.17

Journal homepage: http://sjsutst.polsl.pl

Article citation information:
Vyshnepolskyi, Y., Pavlenko, D., Tumarchenko, L. Innovative approach to ensuring the quality of gas turbine engine parts produced by selective laser sintering for UAV. *Scientific Journal of Silesian University of Technology. Series Transport*. 2024, **124**, 243-260. ISSN: 0209-3324. DOI: https://doi.org/10.20858/sjsutst.2024.124.17.

Yevhen VYSHNEPOLSKYI[1], Dmytro PAVLENKO[2], Larysa TUMARCHENKO[3]

INNOVATIVE APPROACH TO ENSURING THE QUALITY OF GAS TURBINE ENGINE PARTS PRODUCED BY SELECTIVE LASER SINTERING FOR UAV

Summary. The research objects are gas turbine engines parts, manufactured using an innovative method of additive manufacturing – selective laser sintering. The main problem solved in this work is the low quality of the surface layer and the residual porosity of the parts obtained by this method, which significantly limits their operational characteristics and durability. As a result of the experimental studies, rational operating parameters of diamond smoothing were established. This allowed to significantly improve the surface quality and increase the operational characteristics of parts made of heat-resistant alloys INCONEL 718 and an intermetallic alloy based on titanium aluminide OX45-3ODS. The effectiveness of diamond smoothing is explained by local plastic deformation and compaction of the surface layer of parts under the influence of high contact pressures and temperatures. This leads to a significant reduction in surface roughness, an increase in the surface hardness due to strain hardening and a significant reduction in the size and number of residual pores. A characteristic feature of the obtained results is the ability to control the quality parameters of the surface layer by varying

[1] Faculty of Mechanical Engineering, Zaporizhzhia Polytechnic National University, Zhukovsky str. 64, 69063 Zaporizhzhia, Ukraine. Email: evishnepolskiy@gmail.com. ORCID: https://orcid.org/0000-0002-8048-7976
[2] Faculty of Mechanical Engineering, Zaporizhzhia Polytechnic National University, Zhukovsky str. 64, 69063 Zaporizhzhia, Ukraine. Email: dvp1977dvp@gmail.com. ORCID: https://orcid.org/0000-0001-6376-2879
[3] Faculty of Mechanical Engineering, Zaporizhzhia Polytechnic National University, Zhukovsky str. 64, 69063 Zaporizhzhia, Ukraine. Email: hurina97@gmail.com. ORCID: https://orcid.org/0000-0001-7973-7475

the diamond smoothing operating parameters – smoothing force, feed, radius, and geometry of the smoother's working part. The established regularities of the smoothing operating parameters have an impact on the quality characteristics of the surface. This information can be utilized in the development of highly efficient technological processes for the production and restoration of gas turbine engines, critical components of unmanned aerial vehicles, obtained through selective laser sintering. Implementing the elaborated technological recommendations will permit broadening the range of goods produced by additive manufacturing and enhancing their capacity and dependability during operation under conditions of cyclical loads and extreme temperatures.

Keywords: selective laser sintering, diamond smoothing, unmanned aerial vehicle, intermetallic alloy, residual porosity, surface roughness, diamond smoother, smoothing operating parameters, smoothing force, local plastic deformation, operational characteristics

1. INTRODUCTION

In the modern world, unmanned aerial vehicles (UAVs) have entered all spheres of human life. Their development causes constant changes in the requirements for their design and quality parameters. At the same time, the UAVs industry is still quite young and the data on the application of certain design solutions is of a non-systematic, fragmented nature. In many areas of UAVs application their cost, speed of production and repair in the field conditions come first. Additive manufacturing has become widespread to solve referred problems, which allows deploying the production and repair of UAV parts in a small space from almost any material. However, the features of additive manufacturing and the lack of systematic data limit their application [1]. Until recently, the application of additive manufacturing was limited to the production of prototypes and samples for exhibitions

Currently the application percentage of heavy UAVs for reusable and disposable use is increasing exponentially, in which gas turbine engines (GTE) have become widespread [2]. This leads to the formation of new technical requirements that impose on propulsion systems [3]. The characteristics of reusable gas turbine engines correlate with those of manned vehicles, so disposable UAVs allow the application of propulsion systems with a limited-service life, without requiring their repair and high reliability requirements. This significantly changes the approach to development and allows the application of new non-traditional approaches, methods, and technologies in production. A resource of 50 to 250 hours may be sufficient for disposable UAV propulsion systems. This makes it possible to use new technologies that are not yet sufficiently developed for traditional aircraft construction but can significantly reduce installation costs [4]. It is worth mentioning here that in the case of the traditional approach, modern non-invasive diagnostic techniques make it possible to significantly reduce the risk of serious and costly failures [5, 6].

The use of materials with improved physical and mechanical properties [7], as well as new technologies for processing semifinished products [8] and the surface layer [9, 10] for the production of GTE propulsion system parts, has made it possible to significantly improve their characteristics. Among the materials used for the manufacture of gas turbine engine parts, heat-resistant nickel alloys and alloys based on titanium aluminides are widely used. Alloys based on titanium aluminides (TiAl) are of considerable interest in engineering industries that require

low weight and a high strength-to-weight ratio [11]. However, their use is limited by the high cost and difficulties in manufacturing parts from these materials.

Additive manufacturing technologies have become widespread, among which selective laser sintering (SLS) has become widespread to solve these problems.

The main advantage of using SLS for the production of UAV propulsion system parts is the implementation of unattainable or difficult-to-achieve technological production tasks. The modern development of SLS technology has many advantages compared to traditional technologies for producing parts (Fig. 1).

However, despite all the advantages, there are numerous disadvantages that hinder their spread, especially their influence affects the production of GTE critical parts (Fig. 1).

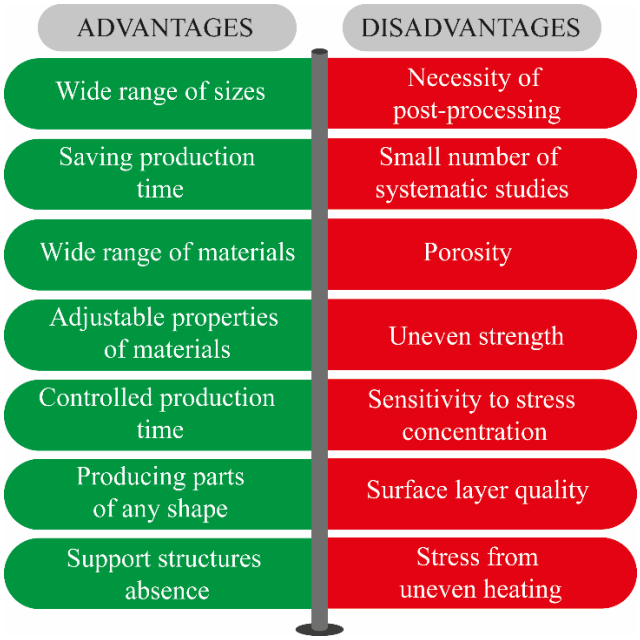

Fig. 1. Advantages and disadvantages of SLS

Many modern studies are devoted to eliminating the factors hindering the development of additive manufacturing technologies. Thus, one of the effective approaches to reducing residual porosity is the use of dispersion strengthening with yttrium oxides [12]. During the synthesis of a part, it is possible to regulate the level of porosity from the core of the sample to its surface by changing the printing modes [13, 14]. However, this leads to an increase in printing time and complicates the process, since it requires studying the influence of selective laser sintering printing parameters on residual porosity. The use of fine-grain powders helps to significantly reduce residual porosity [15]. At the same time, gas atomization is increasingly being used to obtain fine-grain powders. This method makes it possible to obtain a powder with a fraction of 10–80 microns [16, 17], but at the same time significantly increases their cost.

Many studies conducted in different countries are devoted to reducing the cost of titanium alloys powder. One of the approaches is the use of dehydration to obtain non-spherical powders of titanium alloys, which are superior to spherical ones in some parameters [18, 19]. However, this may lead to a decrease in the strength characteristics of the material. For industrial application, it is important to solve the issues of powder distribution in a limited volume and the features of moving non-spherical powder during SLS process.

Hot isostatic pressing is one of the effective methods for reducing residual porosity, but its application is limited by high cost and the possibility of use only for materials with internal pores [20, 21]. For example, its application on INCONEL 718 alloy samples resulted in a significant reduction in the number of internal pores [22]. The study [23] showed that the use of hot isostatic pressing for the TA15 intermetallic alloy led to a decrease in strength characteristics while increasing ductility and toughness.

Unsolved factors limiting the spread of SLS technology in the production of parts is a significant reduction in the characteristics of the surface layer and the negative impact of residual porosity in the presence of structural stress concentrators in the geometry of parts.

A promising solution that will expand the application scope of SLS in the production of gas turbine engine parts is local plastic deformation by diamond smoothing (DS). The peculiarities of the plastic deformation processes occurring in the surface layer during DS make it possible to effectively use it to reduce residual porosity and increase the mechanical characteristics of stress concentration areas in gas turbine engine parts producing by SLS. For example, manufactured by selective laser sintering from an alloy based on titanium aluminide OX45–3ODS and nickel alloy INCONEL 718.

For today, the issue of expanding the application scope of additive manufacturing technologies and improving the surface layer quality of parts made of nickel alloys and alloys based on titanium aluminide, produced by selective laser sintering, is an urgent scientific and applied task.

2. MATERIALS AND METHODS

The following materials were selected for research: heat-resistant alloy 07Cr12NMBFh, titanium aluminide-based alloy OX45-3ODS and nickel alloy INCONEL 718. The characteristics of the materials under study are shown in Table 1.

Tab. 1

Mechanical characteristics of the researched materials

Material	Density, ρ, g/sm3	Young's modulus, E, GPa	Yield strength, $\sigma_{0,2}$, MPa	Tensile strength, σ_B, MPa
07Cr12NMBFh	7,77	194	785	930
INCONEL 718	7,94	173	960	1075
OX45-3ODS	4,4	130	795	970

The samples were obtained by selective laser sintering. In the study of the influence of diamond smoothing operating parameters on the residual porosity and the surface layer quality used standard (Fig. 2 a) and specially designed samples (Fig. 2 b, c).

Standard diamond smoothers were used for hardening, in which the angle of the holder cone was reduced to 75°. To control quality parameters, the following were used: TAYLOR HOBSON profilometer to measure roughness; Vickers microhardness tester model HVA-1 with an indenter load of 100 g and a load time of 30 s to measure the degree of strain hardening. The study of porosity parameters was carried out based on the analysis of metallographic thin sections images using Image Pro Plus software.

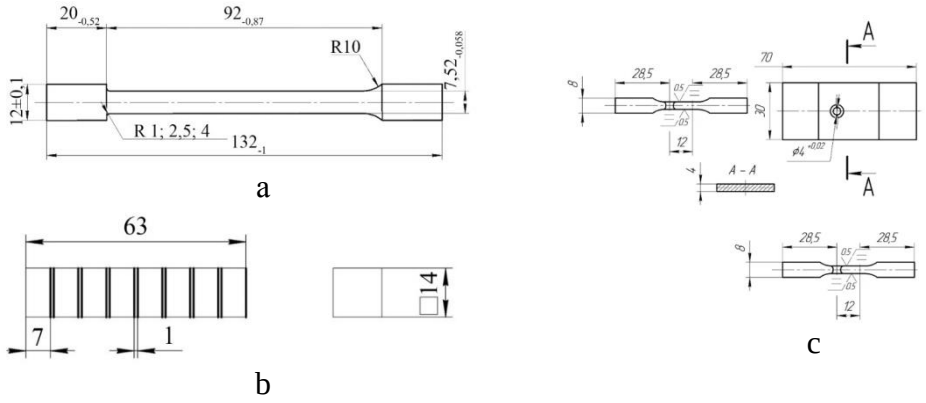

Fig. 2. Geometry of samples for research

3. RESULT AND DISCUSSION

The research on the influence of diamond smoothing operating parameters on the surface layer quality of parts made of 07Cr12NMBFh alloy will make it possible to determine their rational combination, at which minimum roughness is achieved. This study will make it possible to establish the nature of the operating parameters' influence on the hardening of the surface layer, which in turn will significantly reduce the required number of studies required to study the effect of diamond smoothing of parts obtained using SLS, since this alloy is close in characteristics to the studied INCONEL 718.

For this purpose, a full factorial experiment with a 3k design was carried out at k=3; the planning matrix and response function values are shown in Table. 2. The following factors were chosen as varying factors: force, feed and smoothing speed. The standard deviation of the profile was chosen as the objective function.

Tab. 2

Operating parameters and roughness Ra after diamond smoothing of samples from alloy 07Cr12NMBFh

№	F, (H)	S, (mm/rev)	v, (m/min)	Ra, (μm)	№	F, (H)	S, (mm/rev)	v, (m/min)	Ra, (μm)
1	200	0,03	37	0,59	15	300	0,05	145	0,33
2	200	0,03	92	0,50	16	300	0,07	37	0,36
3	200	0,03	145	0,48	17	300	0,07	92	0,25
4	200	0,05	37	0,47	18	300	0,07	145	0,23
5	200	0,05	92	0,38	19	400	0,03	37	0,86
6	200	0,05	145	0,35	20	400	0,03	92	0,70
7	200	0,07	37	0,42	21	400	0,03	145	0,69
8	200	0,07	92	0,38	22	400	0,05	37	0,65
9	200	0,07	145	0,32	23	400	0,05	92	0,55
10	300	0,03	37	0,52	24	400	0,05	145	0,53
11	300	0,03	92	0,41	25	400	0,07	37	0,42

12	300	0,03	145	0,37	26	400	0,07	92	0,36
13	300	0,05	37	0,56	27	400	0,07	145	0,38
14	300	0,05	92	0,35					

It was found that the smoothing speed did not have a statistically significant effect on the roughness of the surface layer, which confirmed the data obtained by researchers for other materials. Figure 3 shows the influence of diamond smoothing operating parameters on the surface roughness of the samples.

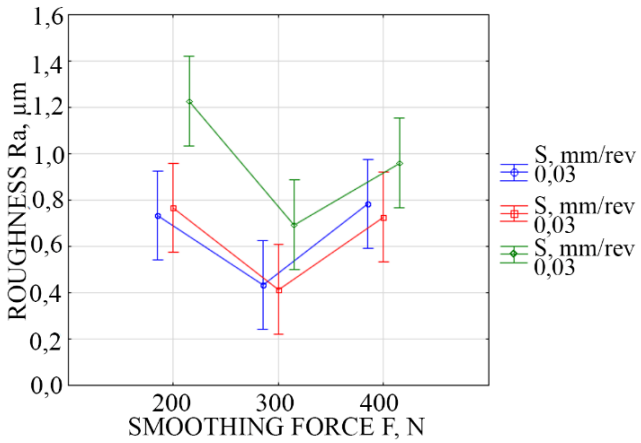

Fig. 3. Influence of diamond smoothing operating parameters on the surface roughness of samples

It was established that smoothing with forces greater than 300 N was not rational, as the roughness deteriorated. This can be explained by the exhaustion of plasticity in the surface layer and the appearance of over-peening.

To assess the phenomena occurring in the surface layer during diamond smoothing, studies were carried out on the operating parameters' influence of the hardening process on the surface layer microstructure of a part made of 07Cr12NMBFh alloy. The microstructure was studied on cross-sections of samples in the initial state and after diamond smoothing with different combinations of operating parameters. Etching of the samples was carried out in a reagent of the following composition: 20 ml HF, 20 ml HNO3, 60 ml H2O. The structure was sorbitol with precipitation of dispersed carbide particles along the boundaries of the original martensite needles (Fig. 4). The release of dispersed carbide particles ensures the stability of defects formed during the martensitic transformation due to phase peening. In high-chromium steels of this class, carbides are identified as M23C6 and VC (1).

In the sample after diamond smoothing according to the operating parameters (F=200 N, v=37 m/min, S=0.03 mm/min) in a shallow surface layer up to 10 µm in-depth, slip lines were revealed in individual grains with a preferred orientation relative to external acting forces (Fig. 5).

Compared to the initial state, the roughness decreased significantly. Increasing the force to 300 - 400 N led to an increase in the depth of the deformed layer to 25 µm and 34 µm, while slip lines were already present in all grains of the surface layer (Fig. 6 a and 6 b).

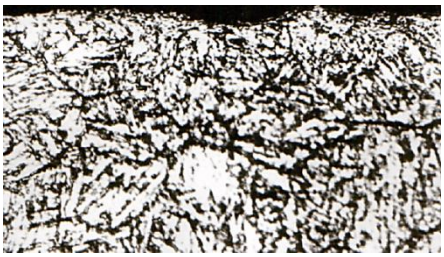

Fig. 4. Microstructure of the original sample

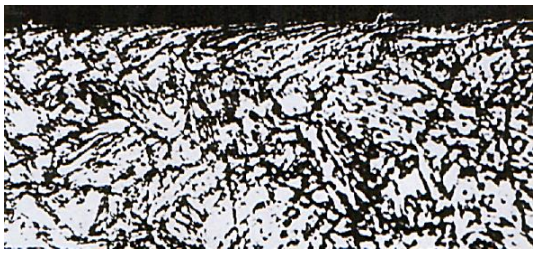

Fig. 5. Microstructure of a sample hardened under operating parameters (F=200N, v=37 m/min, S=0.03mm/min)

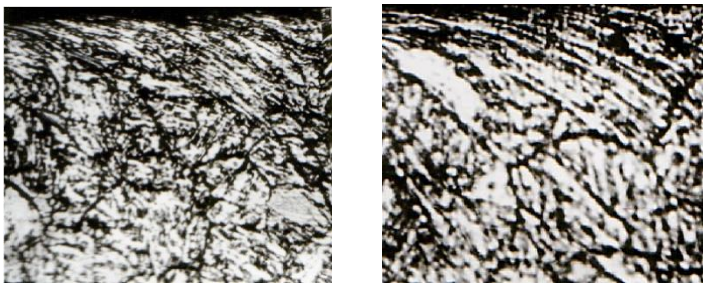

a b

Fig. 6. Microstructure of samples hardened under operating parameters:
a - F=300 N, v=145 m/min, S=0.03 mm/min; b - F=300 N, v=115 m/min, S=0.05 mm/min

Analysis of the microstructure after various diamond smoothing operating parameters allows to presumably explain the detection of changes in the thin surface layer as follows. Within the ferrite grain curved lines of a curvilinear type were observed; they resembled slip lines running in one direction at a certain angle to the surface of the samples, which was associated with a certain characteristic vector of acting forces when the movement of a diamond ball with a diameter of 2.5 mm occurred while the part rotated at a certain speed

Processing of experimental data made it possible to establish that a rational combination of operating parameters at which the minimum roughness was achieved: smoothing force F=300 N; feed S= 0.05 mm/rev; smoothing speed v=115 m/min. The conducted research made it possible to significantly reduce the number of experiments required to study the influence of diamond smoothing operating parameters on the characteristics of the surface and surface layer of parts obtained by SLS from nickel alloys and alloys based on titanium aluminides.

The following were selected as varying factors for samples made of the INCONEL 718 nickel alloy: the sphere radius of the diamond smoother Rsf (1.0; 2.5; 4.0 mm); smoothing force F (0.2; 0.3; 0.4 kN); smoothing feed S (0.05; 0.1; 0.15mm/rev).

A fractional factorial experiment 32-1 was selected to study the influence of operating parameters of diamond smoothing on the characteristics of the surface layer. The standard deviation of the profile Ra, μm and the degree of strain hardening SHμ, % were chosen as the response functions. The values of the variable factors and the resulting response functions are shown in Table 3.

The figure shows an image of a surface layer cross-section of samples hardened by diamond smoothing with combinations of operating parameters at which the maximum degree of strain hardening (№ 2 (Fig. 7 a)) and the minimum roughness (№ 7 (Fig. 6 b)) were obtained.

Tab. 3

Values of variable factors and obtained response functions

№	F (kN)	S (mm/rev)	R_{sf} (mm)	Ra (μm)	$S_{H\mu}$ (%)
1	0,2	0,05	1	1,6	37,04
2	0,3	0,15	1	4,92	59,33
3	0,4	0,10	1	3,82	42,61
4	0,3	0,10	2,5	0,74	45,68
5	0,4	0,05	2,5	0,73	35,38
6	0,2	0,15	2,5	0,88	26,18
7	0,3	0,05	4	0,47	3,89
8	0,4	0,15	4	1,22	8,07
9	0,2	0,10	4	0,62	23,95

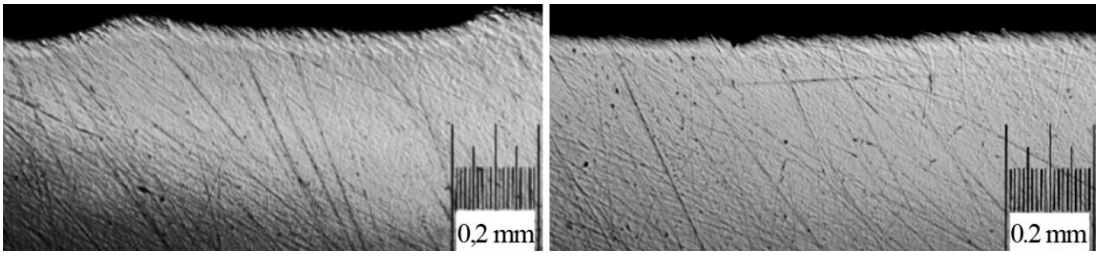

a b

Fig. 7. Image of the surface layer cross-section of samples made of nickel alloy INCONEL 718, hardened by diamond smoothing: a – mode № 2; b – mode № 7 (Table 3)

Compaction of the surface layer was observed on samples after diamond smoothing. Research data showed that to obtain minimum roughness, it was necessary to increase the smoother radius and reduce the feed (mode № 7 (Fig. 7 b)); however, it contradicted the combination of operating parameters at which the maximum degree of strain hardening (mode № 2) was obtained (Fig. 7 a). Therefore, for practical application a compromise is necessary: which is required: low roughness or high degree of strain hardening. If both parameters are important, then it is necessary to use a combination of operating parameters at which both response functions will be rational (mode № 4, Table 3).

Visualization of the influence of diamond smoothing operating parameters on the formation of roughness and the degree of strain hardening is shown in Figure 8.

A rational degree of strain hardening (Fig. 8 a) was achieved by using a smoother with a sphere radius of 1 mm and a maximum smoothing force. At the same time, smoother with a sphere radius of 4 mm and a minimum feed led to achieving minimum roughness (Fig. 8 b). Therefore, the radius of the smoother sphere should be 2.5 mm to simultaneously obtain a rational degree of strain hardening and minimum roughness.

The regression equations were obtained to predict the magnitude of roughness and the degree of strain hardening from various combinations of operating parameters:

$$S_{H\mu} = 600{,}12 - 965 \cdot F + 2183{,}3 \cdot F^2 + 231{,}3 \cdot S^2 + 11{,}5 \cdot R_{sf} - 10{,}5 \cdot R_{sf}^2 \quad (1)$$

$$Ra = 3{,}17 - 5{,}28 \cdot F + 10{,}83 \cdot F^2 + 4{,}1 \cdot S - 1{,}46 \cdot R_{sf} + 0{,}22 \cdot R_{sf}^2 \quad (2)$$

where: *F* – smoothing force, kN;
S – smoothing feed, mm/rev;
Rsf – radius of diamond smoother, mm;
Ra – roughness, μm;
SHμ – degree of strain hardening, %.

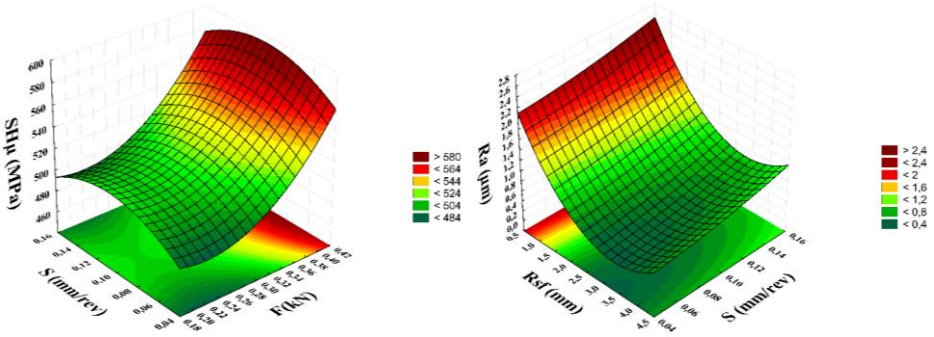

a b

Fig. 8. The influence of operating parameters DS on the degree of strain hardening SHμ (a) and roughness Ra (b)

In order to expand the application scope of additive manufacturing technologies, the study of the influence of diamond smoothing operating parameters on the quality characteristics of parts manufactured using SLS from alloys based on titanium aluminide is an urgent task.

The alloy has low density, high heat resistance and high mechanical properties. The residual porosity of the samples produced by SLS obtained from the OX45-3ODS alloy was at the level of 17-22%. Dead-end pores (Fig. 9) significantly reduced the quality characteristics of parts made of specified alloys.

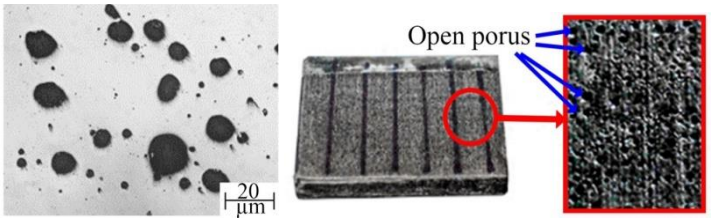

Fig. 9. Microstructure and surface with dead-end pores of the OX45-3ODS alloy sample

A full factorial analysis was performed using three varied factors (Table 4) in order to study the effect of diamond smoothing operating parameters on the surface quality of OX45-3ODS alloy samples.

The original porosity was chosen as the X4 factor, it had no levels of variation, since its distribution was random, and it was entered into the planning matrix as a directly measured value for each sample before diamond smoothing. The standard deviation of the profile Ra (μm) and the degree of strain hardening SHμ, %, were chosen as response functions. The number of possible combinations of factor levels N=27. The planning matrix and the results of the conducted experiment are shown in Table 5.

Tab. 4

Variations of factor levels

Factor	Force F, kN			Feed S, mm/rev			Radius of diamond smoother, R_{sf}, mm		
	X1			X2			X3		
Level	-1	0	+1	-1	0	+1	-1	0	+1
Factor value	0,1	0,3	0,4	0,05	0,1	0,15	1,0	2,5	4,0

Tab. 5

Planning matrix and results of the conducted experiment

№	X1	X2	X3	X4	Ra	$S_{H\mu}$	№	X1	X2	X3	X4	Ra	$S_{H\mu}$
1	-1	-1	-1	0,246	1,10	45	15	0	0	+1	0,16	0,67	47
2	-1	-1	0	0,1233	0,85	47	16	0	+1	-1	0,13	3,87	77
3	-1	-1	+1	0,1866	1,15	34	17	0	+1	0	0,11	1,0	53
4	-1	0	-1	0,13	2,04	24	18	0	+1	+1	0,15	1,35	55
5	-1	0	0	0,1833	1,3	46	19	+1	-1	-1	0,1	2,99	25
6	-1	0	+1	0,1666	1,4	28	20	+1	-1	0	0,15	1,47	53
7	-1	+1	-1	0,1	2,6	34	21	+1	-1	+1	0,16	0,97	58
8	-1	+1	0	0,13	1,25	42	22	+1	0	-1	0,11	2,97	58
9	-1	+1	+1	0,11	1,07	47	23	+1	0	0	0,13	0,68	68
10	0	-1	-1	0,1166	4,26	50	24	+1	0	+1	0,1	1,0	54
11	0	-1	0	0,152	1,27	64	25	+1	+1	-1	0,15	4,15	56
12	0	-1	+1	0,1	1,103	34	26	+1	+1	0	0,12	0,79	53
13	0	0	-1	0,1	3,38	50	27	+1	+1	+1	0,18	0,704	61
14	0	0	0	0,11	0,79	63							

The regularities of the smoothing operating parameters' impact on roughness were subject to the polynomial distribution law. Polynomial surfaces most accurately approximated the regularities of influence on roughness: the smoothing feed and the radius of the smoother sphere (Fig. 10). The combination of these factors had the greatest effect on the roughness of the hardened surface. The established regularities showed that for smoothing of porous materials it was necessary to use a diamond smoother with a radius of the diamond sphere equalled more than 2.5 mm. A smoother with a smaller radius, hitting the dead-end pores, leading to a deterioration of the surface roughness due to its cracking.

Due to the fact that the studied material has high-strength characteristics, its smoothing with a force of less than 0.3 kN is impractical, since it does not lead to a sufficient degree of deformation at the point of contact. The rational value of feed for smoothing the studied alloy was 0.1 mm/rev. A larger feed led to an insufficient degree of overlap of the grooves after smoothing, a smaller one, due to the insufficient plasticity of the material, led to the destruction of the already hardened surface due to the passage of the smoother over the hardened surface.

Increasing the wear resistance of the part surface, which is affected by the degree of strain hardening, is important for improving the quality of parts. According to the data obtained during the multifactorial experiment (Table 4 and 5), dependencies (Fig. 11) were constructed, which showed the effect on the degree of strain hardening of various operating parameters of diamond smoothing: feed, the radius of the diamond smoother sphere and initial porosity.

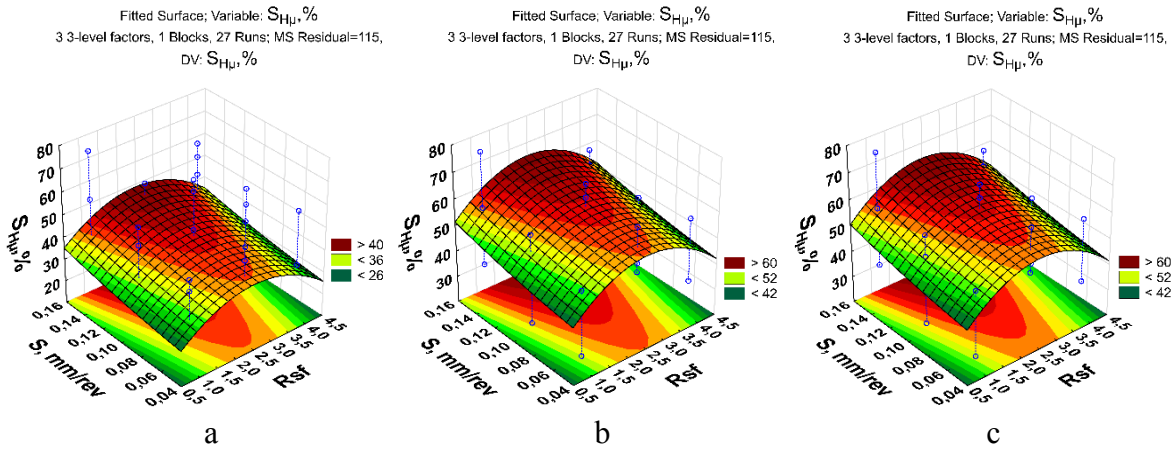

Fig. 10. Dependencies of surface roughness on DS parameters:
a – F=0.1kN; b – F=0.3 kN; c – F=0.4 kN

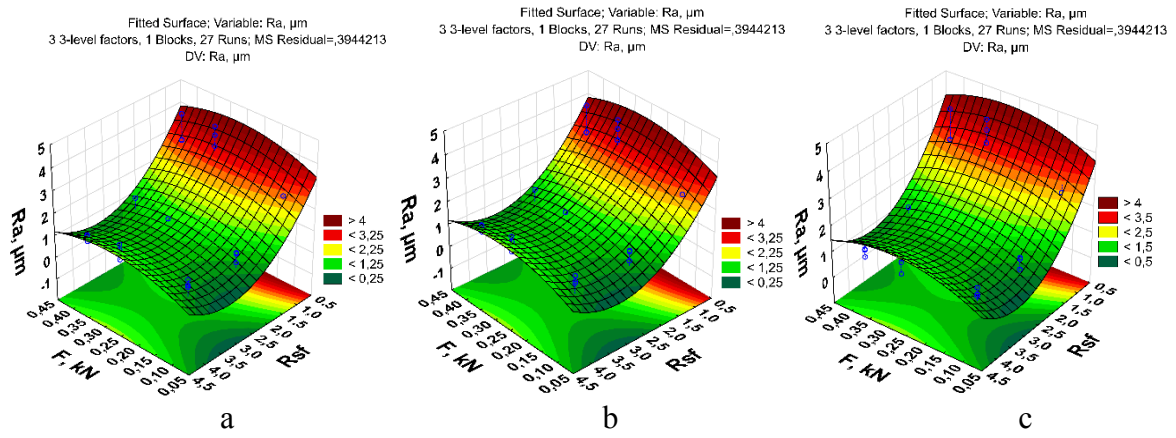

Fig. 11. Dependencies of the degree of strain hardening on the operating parameters of diamond smoothing: a – S=0.05mm/rev; b – S=0.1mm/rev; c – S=0.15mm/rev

Determining the significance of diamond smoothing operating parameters in the formation of the degree of strain hardening of alloys based on titanium aluminides OX45-3ODS was performed by variance analysis (Table 6) based on the conducted full-factor experiment.

The variance analysis (Table 6) showed that the smoothing force and its combination, to a certain extent, with the smoothing feed had the greatest influence on the degree of strain hardening. A regression analysis (Table 7) was performed to develop a mathematical model that allowed predicting the degree of strain hardening from different combinations of operating parameters.

Tab. 6

The variance analysis of the degree of strain hardening of the alloy based on titanium aluminides OX45-3ODS after diamond smoothing

Factor	SS	df	MS	F	P
F(L)	0,147226	1	0,147226	21,49915	0,000159
(2)s(L)	0,025689	1	0,025689	3,75129	0,067023
r(Q)	0,031296	1	0,031296	4,57013	0,045066
1Lby2Q	0,040899	1	0,040899	5,97245	0,023927
1Qby3L	0,055225	1	0,055225	8,06438	0,010124
2Lby3Q	0,037378	1	0,037378	5,45819	0,029998
Error	0,136960	20	0,006848		
Total variance	0,474674	26			

Tab. 7

Regression analysis of the change in the degree of strain hardening from different combinations of diamond smoothing operating parameters

Factor	Regression coefficients	Error	t(14)	p	The lower limit of the confidence interval	The upper limit of the confidence interval
Free factor	0,617	0,1986	3,10569	0,007744	0,191	1,043
(1)f(L)	5,907	1,5021	3,93250	0,001503	2,685	9,129
f(Q)	-17,217	3,5587	-4,83804	0,000263	-24,850	-9,585
(2)s(L)	-26,537	5,7237	-4,63629	0,000385	-38,813	-14,261
S(Q)	154,164	32,1935	4,78866	0,000289	85,116	223,212
1Qby2L	121,953	39,7843	3,06535	0,008390	36,624	207,281
1Qby2Q	-567,653	196,8812	-2,88323	0,012034	-989,921	-145,385
1Lby3L	-1,629	0,5195	-3,13654	0,007284	-2,744	-0,515
1Qby3L	3,636	1,0801	3,36612	0,004614	1,319	5,952
2Lby3L	13,132	2,8874	4,54818	0,000455	6,939	19,325
2Lby3Q	-2,021	0,5273	-3,83250	0,001830	-3,152	-0,890
2Qby3L	-87,932	20,8773	-4,21182	0,000870	-132,709	-43,154
2Qby3Q	14,534	3,9864	3,64596	0,002646	5,984	23,084

Based on the determined regression coefficients, a regression equation was established that allowed predicting the degree of strain hardening from different combinations of diamond smoothing operating parameters:

$$S_{H\mu} = 0{,}6 + 5{,}9 \cdot F - 17{,}2 \cdot F^2 - 26{,}5 \cdot S + 154{,}2 \cdot S^2 + 121{,}9 \cdot F^2 \cdot S - 567{,}6 \cdot F^2 \cdot S^2 - 1{,}6 \cdot F \cdot R_{sf} + 3{,}6 \cdot F^2 \cdot R_{sf} + 13{,}1 \cdot S \cdot R_{sf} - 2 \cdot S \cdot R_{sf}^2 - 87{,}9 \cdot S^2 \cdot R_{sf} + 14{,}5 \cdot S^2 \cdot R_{sf}^2 \quad (3)$$

The adequacy of the obtained regression equation was checked on the basis of the predicted values to the observed values correspondence graph (Fig. 12).

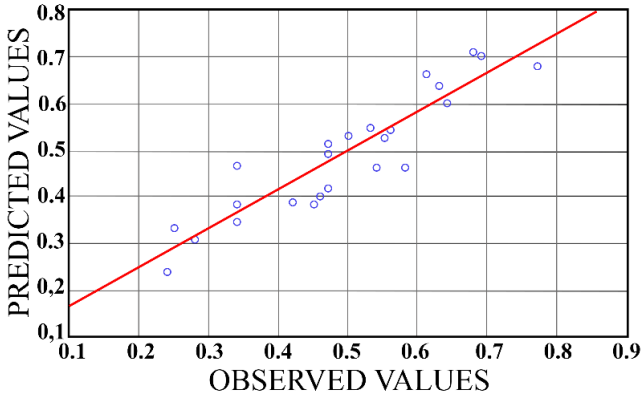

Fig. 12. Correspondence of predicted values to observed values

The predicted values (Fig. 12) did not have a high discrepancy with the values obtained experimentally, accordingly, the obtained regression equation had sufficient adequacy and could be used to predict the magnitude of the degree of strain hardening depending on one or another combination of operating parameters.

One of the main disadvantages of powder metallurgy and additive manufacturing is residual porosity, which contributes to a decrease in strength, plasticity, fracture toughness, crack resistance, and machinability, and also leads to a decrease in tribotechnical characteristics. The shape of the pores, characterized by their perimeter, greatly influences the probability of cracks occurring. The value of the pore perimeter after diamond smoothing with different combinations of operating parameters is shown in Table 8.

Tab. 8

Operating parameter modes of diamond smoothing of OX45-3ODS alloy samples

№	P	№	P	№	P	№	P	№	P	№	P	№	P
1	1,6722	5	1,3844	9	1,4902	13	0,3852	17	0,6518	21	1,5944	25	2,2129
2	1,1826	6	1,2334	10	1,2704	14	0,4806	18	0,6824	22	1,3090	26	1,8112
3	1,7999	7	1,3076	11	2,8276	15	1,0208	19	1,1784	23	1,2643	27	2,2513
4	0,9925	8	2,1066	12	2,1411	16	0,9533	20	1,2476	24	2,0286		

The influence of diamond smoothing on the pores and their perimeter in the surface layer of a sample hardened by diamond smoothing with rational operating parameters is shown in Figure 13.

The analysis of the experiment results using Pareto diagrams allowed establishment of the influence of the smoothing operating parameters and their interactions on the perimeter of the pores in the surface layer (Fig. 14).

It was found that the greatest influence had the combined effect of the feed and the smoothing force. A regression analysis was carried out (Table 9) in order to obtain a regression equation that would allow predicting the influence of diamond smoothing operating parameters on the perimeter of residual pores in the surface layer.

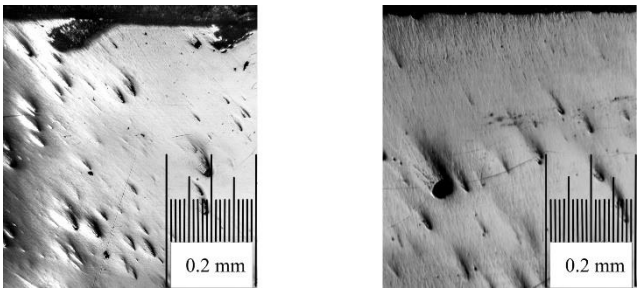

a b

Fig. 13. The surface layer of samples from an alloy based on titanium aluminide:
a - initial sample; b - Mode № 14 (Table 5)

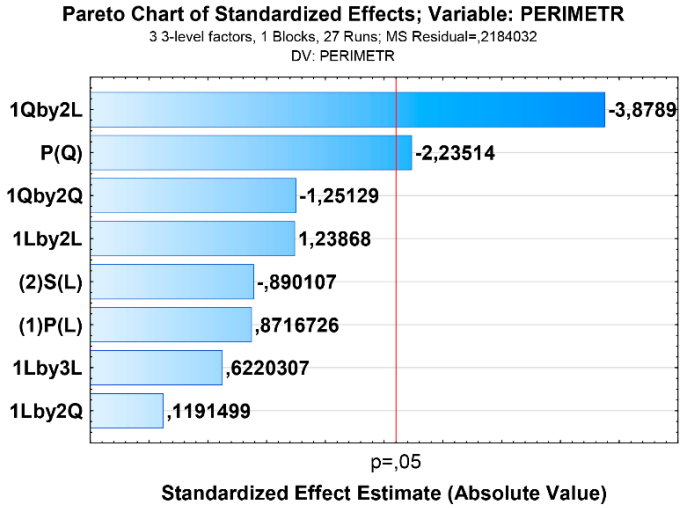

Fig. 14. Pareto diagram for the model of the diamond smoothing operating parameters influence on the perimeter of the pores in the surface layer

Tab. 9

Regression analysis of the diamond smoothing operating parameters' influence on the perimeter of residual pores in the surface layer of titanium aluminide-based alloy parts

Factor	Regr. Coefficients; Var.:PERIMETER; R-sqr=,74238; Adj:, 3 3-level factors, 1 Blocks, 27 Runs; MS Residual=,1282098 DV: PERIMETER					
	Regressn Coeff.	Std. Err.	t(18)	p	-95,% Cnf.Limt	+95,% Cnf.Limt
MEAN/Intarc.	-1,28	0,947	-1,35615	0,191821	-3,3	0,706
(1)P(L)	55,53	12,968	4,28201	0,000449	28,3	82,771
P(Q)	-122,30	30,974	-3,94846	0,000942	-187,4	-57,225
(2)S(L)	35,53	8,771	4,05044	0,000751	17,1	53,952
1L by 2L	-985,88	225,444	-4,37308	0,000367	-1459,5	-512,245
1L by 2Q	2733,26	1034,407	2,64234	0,016555	560,0	4906,466
1Q by 2L	2164,05	602,055	3,59444	0,002073	899,2	3428,917
1Q by 2Q	-6205,10	2868,929	-2,16286	0,044256	-12232,5	-177,703
1L by 3L	0,38	0,191	2,00200	0,060587	-0,0	0,784

A regression equation was obtained that allowed predicting the perimeter of residual pores from different combinations of diamond smoothing operating parameters:

$$PERIMETR = -1{,}28 + 55{,}53 \cdot F + 122{,}30 \cdot F^2 + 35{,}53 \cdot S - 985{,}88 \cdot F \cdot S + 2733{,}26 \cdot F \cdot S^2 + 2164{,}05 \cdot F^2 \cdot S - 6205{,}1 \cdot F^2 \cdot S - 2164{,}05 \cdot F^2 \cdot S - 6205{,}1 \cdot F^2 \cdot S^2 + 0{,}38 \cdot F \cdot R_{sf} \quad (4)$$

It was established that the dependencies of the residual pores' perimeter in the surface layer on the force and smoothing feed for different radii of the smoother were of an extreme nature (Fig. 15).

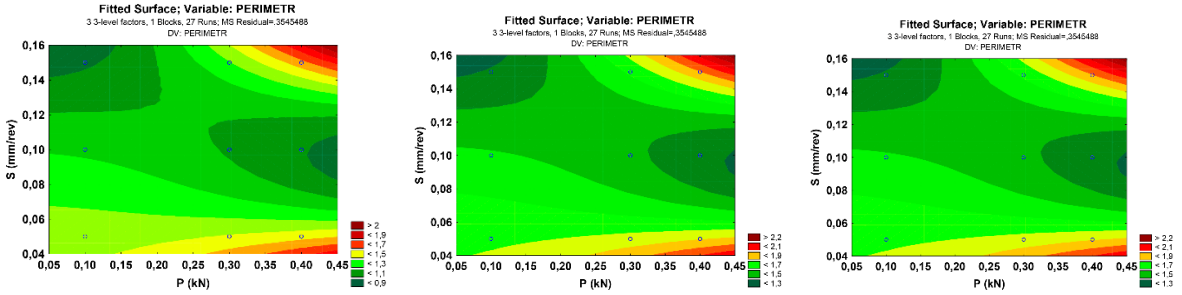

a b c

Fig. 15. Effect of force and feed on porosity during processing with different smoothers: a – Rsf = 1 mm; b – Rsf = 2.5 mm; c – Rsf = 4 mm

A rational combination of operating parameters was smoothing with a force of 0.2-0.3 kN, with a feed of 0.12-0.15 mm/rev. The minimum values of the pore perimeter were obtained when using a smoother with a radius of 1 mm, however, as already mentioned, its applying led to cracking of the surface (Fig. 15 a). It follows from the above that the rational radius of the smoother is 2.5 mm (Fig. 15 b). The use of a smoother with a radius of 4 mm (Fig. 15 c) led to a significant increase in specific contact pressure, which led to deformation during processing of a thin-walled part.

The response surface built on the basis of a nonlinear regression model was evaluated in order to find the rational smoothing operating parameters, ensuring the minimum residual porosity. The assessment was performed by the Box-Wilson steep ascent method (Table 10).

Tab. 10

Rational modes obtained based on the analysis of the response surface by the Box-Wilson steep ascent method

Factor	Minimum	Rational values	Maximum
Area of residual pores, P, %			
F, kN	0,10	0,21	0,40
S, mm/rev	0,05	0,11	0,15
R_{sf}, mm	1,00	4,60	4,00

Considering the possible design limitations of real thin-walled parts, the rational diamond smoother is 2.5 mm to ensure the best result. The rational smoothing force is 0.22 - 0.3 kN. The rational feed is 0.1 mm/rev, but this parameter may change depending on the equipment used, in this case it is necessary to take as close as possible to the established value.

4. CONCLUSION

In order to expand the application scope of additive manufacturing technologies and improve the surface layer quality of parts made of nickel alloys and alloys based on titanium aluminide, produced using selective laser sintering, an innovative approach to improving their quality was proposed. It is based on the application of surface layer local deformation treatment of the part's structural stress concentrators by diamond smoothing. It was established that the main problems that hindered the spread of additive technologies in production were porosity, powder cost, uniformity, sensitivity to stress concentration and surface layer quality. The influence of the diamond smoothing operating parameters on the formation of surface quality characteristics, the degree of strain hardening, the distribution of residual stresses and fatigue resistance during machining parts made of 07Cr12NMBFh alloy were determined. A rational combination of operating parameters for diamond smoothing of the mentioned material: smoothing force F=300 N; feed rate S=0.05 mm/rev; smoothing speed v=115 m/min.

The main regularities of the quality parameters formation of the treated surface and surface layer depending on the diamond smoother parameters for parts obtained by selective laser sintering from an alloy based on titanium aluminides OX45-3ODS and heat-resistant nickel alloy INCONEL 718 were determined. The rational diamond smoothing operating parameters of the samples made of titanium aluminide-based alloy OX45-3ODS were smoothing with a force of 300 N, feed rate of 0.1 mm/rev and a diamond smoother with a radius of 2.5 mm. The diamond smoothing operating parameters had a different effect on the roughness and degree of strain hardening of the surface layer of INCONEL 718 alloy samples. The expedient combination of these parameters, in which the degree of strain hardening and roughness were rational, was machining with a smoothing force of 250 N, feed rate of 0.1 mm/rev and a diamond smoother sphere radius of 2.5 mm.

The effect of technological features of processing and operating parameters of diamond smoothing on the perimeter of residual pores in the surface layer was determined. The most significant parameter in the study of the effectiveness of diamond smoothing for hardening materials obtained by selective laser sintering was the residual porosity. The minimum values of the residual pore perimeters were achieved by diamond smoothing with the following operating parameters: force 0.2-0.3 kN, feed rate 0.12-0.15 mm/rev and diamond smoothing sphere radius 2.5 mm.

References

1. Goh, G.D., S. Agarwala, G.L. Goh, V. Dikshit, S.L. Sing, W.Y. Yeong. 2017. „Additive manufacturing in unmanned aerial vehicles (UAVs): Challenges and potential”. *Aerospace Science and Technology* 63: 140-151. DOI: https://doi.org/10.1016/j.ast.2016.12.019.

2. Zhang B., Z. Song, F. Zhao, C. Liu. 2022. „Overview of propulsion systems for unmanned aerial vehicles". *Energies* 15(2): 455. DOI: https://doi.org/10.3390/en15020455.
3. Balli O., H. Caliskan. 2021. „On-design and off-design operation performance assessments of an aero turboprop engine used on unmanned aerial vehicles (UAVs) in terms of aviation, thermodynamic, environmental and sustainability perspectives". *Energy Conversion and Management* 243: 114403. DOI: https://doi.org/10.1016/j.enconman.2021.114403.
4. Clark I. 2005. „Limited life engines for UAVs". *The Aeronautical Journal* 109(1095): 247-254. DOI: https://doi.org/10.1017/S0001924000005224.
5. Czech Piotr. 2012. „Identification of Leakages in the Inlet System of an Internal Combustion Engine with the Use of Wigner-Ville Transform and RBF Neural Networks". Communications in Computer and Information Science 329: 175-182. DOI: https://doi.org/10.1007/978-3-642-34050-5_47. Springer, Berlin, Heidelberg. ISBN: 978-3-642-34049-9; 978-3-642-34050-5. ISSN: 1865-0929. In: Mikulski Jerzy (eds), Telematics in the transport environment, 12th International Conference on Transport Systems Telematics, Katowice Ustron, Poland, October 10-13, 2012.
6. Czech Piotr. 2011. „Diagnosing of disturbances in the ignition system by vibroacoustic signals and radial basis function - preliminary research". Communications in Computer and Information Science 239: 110-117. DOI: https://doi.org/10.1007/978-3-642-24660-9_13. Springer, Berlin, Heidelberg. ISBN: 978-3-642-24659-3. ISSN: 1865-0929. In: Mikulski Jerzy (eds), Modern transport telematics, 11th International Conference on Transport Systems Telematics, Katowice Ustron, Poland, October 19-22, 2011.
7. Altıparmak S.C., B. Xiao. 2021. „A market assessment of additive manufacturing potential for the aerospace industry". *Journal of Manufacturing Processes* 68: 728-738. DOI: https://doi.org/10.1016/j.jmapro.2021.05.072.
8. Karpinos B.S., D.V. Pavlenko, O.Ya. Kachan. 2012. „Deformation of a submicrocrystalline vt1-0 titanium alloy under static loading". *Strength of Materials* 44: 100-107. DOI: https://doi.org/10.1007/s11223-012-9354-9.
9. Vyshnepolskyi Y., D. Pavlenko, D. Tkach. 2020. „Parts Diamond Burnishing Process Regimes optimization Made of INCONEL718 Alloy via Selective Laser Sintering Method". In: *Proceedings of the 2020 IEEE 10th International Conference on "Nanomaterials: Applications and Properties". NAP 2020*. DOI: https://doi.org/10.1109/NAP45177.2020.9309661.
10. Pavlenko D., E. Kondratiuk, Y. Torba, Y. Vyshnepolskyi, D. Stepanov. 2022. „Improving the efficiency of finishing-hardening treatment of gas turbine engine blades". *Eastern-European Journal of Enterprise Technologies*. DOI: https://doi.org/10.15587/1729-4061.2022.252292.
11. Tshephe T.S., S.O. Akinwamide, E. Olevsky, P.A. Olubambi. 2022. „Additive manufacturing of titanium-based alloys- A review of methods, properties, challenges, and prospects". *Heliyon* 8(3): e09041. DOI: https://doi.org/10.1016/j.heliyon.2022.e09041.
12. Li W.P., H. Wang, Y.H. Zhou, Y.Y. Zhu, S.F. Lin, M. Yan, N. Wang. 2022. „Yttrium for the selective laser melting of Ti-45Al-8Nb intermetallic: Powder surface structure, laser absorptivity, and printability". *Journal of Alloys and Compounds* 892: 161970. DOI: https://doi.org/10.1016/j.jallcom.2021.161970.
13. Ahmad S., S. Mujumdar, V. Varghese. 2022. "Role of porosity in machinability of additively manufactured Ti-6Al-4V". *Precision Engineering* 76: 397-406. DOI: https://doi.org/10.1016/j.precisioneng.2022.04.010.

14. Kaschel F.R., M. Celikin, D.P. Dowling. 2020. „Effects of laser power on geometry, microstructure and mechanical properties of printed Ti-6Al-4V parts". *Journal of Materials Processing Technology* 278: 116539. DOI: https://doi.org/10.1016/j.jmatprotec.2019.116539.
15. Moghimian P., T. Poirié, M. Habibnejad-Korayem, J.A. Zavala, J. Kroeger, F. Marion, F. Larouche. 2021. „Metal powders in additive manufacturing: A review on reusability and recyclability of common titanium, nickel and aluminum alloys". *Additive Manufacturing* 43: 102017. DOI: https://doi.org/10.1016/j.addma.2021.102017.
16. Cacace S., M. Boccadoro, Q. Semeraro. 2023. "Investigation on the effect of the gas-to-metal ratio on powder properties and PBF-LB/M processability". *Progress in Additive Manufacturing* 9: 889-904. DOI: https://doi.org/10.1007/s40964-023-00490-z.
17. Soong S.Z., W.L. Lai, A.N. Kay Lup. 2023. „Atomization of metal and alloy powders: Processes, parameters, and properties". *AIChE Journal* 69(11): e18217. DOI: https://doi.org/10.1002/aic.18217.
18. Dong S., G. Ma, P. Lei, T. Cheng, D. Savvakin, O. Ivasishin. 2021. "Comparative study on the densification process of different titanium powders". *Advanced Powder Technology* 32(7): 2300-2310. DOI: https://doi.org/10.1016/j.apt.2021.05.009.
19. Delpazir M.H., M. Asherloo, S.N.K. Abad, A. Thompson, V. Guma, S.D. Bagi, A. Mostafaei. 2023. „Microstructure and corrosion behavior of differently heat-treated Ti-6Al-4V alloy processed by laser powder bed fusion of hydride-dehydride powder". *Corrosion Science* 224: 111495. DOI: https://doi.org/10.1016/j.corsci.2023.111495.
20. Ng C.H., M.J. Bermingham, M.S. Dargusch. 2023. "Eliminating porosity defects, promoting equiaxed grains and improving the mechanical properties of additively manufactured Ti-22V-4Al with super-transus hot isostatic pressing". *Additive Manufacturing* 72: 103630. DOI: https://doi.org/10.1016/j.addma.2023.103630.
21. Zhang M., C.H. Ng, A. Dehghan-Manshadi, C. Hall, M.J. Bermingham, M.S. Dargusch. 2023. "Towards isotropic behaviour in Ti-6Al-4V fabricated with laser powder bed fusion and super transus hot isostatic pressing". *Materials Science and Engineering: A* 874: 145094. DOI: https://doi.org/10.1016/j.msea.2023.145094.
22. Marques A., Â. Cunha, F. Bartolomeu, F.S. Silva, Ó. Carvalho. 2023. "Inconel 718 produced by hot pressing: optimization of temperature and pressure conditions". *The International Journal of Advanced Manufacturing Technology* 128(1-2): 891-901. DOI: https://doi.org/10.1007/s00170-023-11950-9.
23. Zhu L., Y. Pan, Y. Liu, Z. Sun, X. Wang, H. Nan, X. Lu. 2023. „Effects of microstructure characteristics on the tensile properties and fracture toughness of TA15 alloy fabricated by hot isostatic pressing". *International Journal of Minerals, Metallurgy and Materials* 30(4): 697-706. DOI: https://doi.org/10.1007/s12613-021-2371-6.

Received 18.05.2024; accepted in revised form 30.07.2024